

## Perfect transfer of path-entangled photons in $J_x$ photonic lattices

Armando Perez-Leija,<sup>1,\*</sup> Robert Keil,<sup>2</sup> Hector Moya-Cessa,<sup>1,3</sup> Alexander Szameit,<sup>2</sup> and Demetrios N. Christodoulides<sup>1</sup>

<sup>1</sup>CREOL/College of Optics, University of Central Florida, Orlando, Florida, USA

<sup>2</sup>Institute of Applied Physics, Friedrich-Schiller Universität Jena, Max-Wien-Platz 1, 07743 Jena, Germany

<sup>3</sup>INAOE, Coordinación de Óptica, Luis Enrique Erro No. 1, 72840 Toantzintla, Puebla, Mexico

(Received 4 October 2012; published 4 February 2013)

We demonstrate that perfect transfer of path-entangled photons as well as of single-photon states is possible in a certain class of spin inspired optical systems—the so-called  $J_x$  photonic lattices. In these fully integrable optical arrangements, perfect cyclic transitions from correlated states to totally anticorrelated states can naturally occur. Moreover we show that the bunching and antibunching response of path-entangled photons can be preengineered at will in such coupled optical arrangements. We elucidate these effects via pertinent examples.

DOI: [10.1103/PhysRevA.87.022303](https://doi.org/10.1103/PhysRevA.87.022303)

PACS number(s): 03.67.Hk, 42.50.Ex, 05.60.Gg, 42.82.Et

### I. INTRODUCTION

Coherent transfer of quantum information between distant ports or nodes is a crucial task within the framework of quantum computing and information processing. Over the years, several physical platforms have been suggested in order to attain such a state transfer. These include, for example, spin chains, arrays of quantum dots, coupled cavities, etc. [1–4]. In this regard, various studies have revealed that spin chains interacting via specially engineered Heisenberg Hamiltonians can effectively achieve a perfect delivery of fermionic quantum states from one vertex of the chain to the other [5,6]. In fact, the hopping parameters involved in these spin systems are identical to the matrix elements of the  $J_x$  quantum angular momentum operator, i.e., they obey a parabolic distribution [5]. In Hilbert space, these spin chains act as quantum rotations of the input states. By their very nature, approaches based on spin chains present several intrinsic advantages and disadvantages. On the one hand, they offer a versatile environment for quantum communications over short distances, they allow for simultaneous operations on several qubits, and they are also useful for long-time qubit storage [6,7]. On the other hand, since the spin “links” are closely spaced so as to enable strong spin-spin interactions, they are plagued with difficulties in addressing individual qubits [8].

Optics, on the other hand, offers long coherence times due to negligible photon interactions and a high degree of experimental control [9]. As we elucidate in this paper, perfect transfer via photonic lattices is not only possible for states residing on single sites, but for any multimode input state, separable or entangled. In addition, the properties of these waveguide arrays can also be exploited for classical light [10–14], showing revivals of extended wave packets and discrete focusing.

This paper is organized as follows: Section II is devoted to investigating the evolution dynamics of single-photon states in  $J_x$  photonic lattices. Furthermore, we examine the perfect transfer of entangled multipartite  $W$  states. In Sec. III we analyze the perfect transfer of spatially extended correlated and anticorrelated path-entangled photon states by monitoring the respective quantum correlation maps. For completeness sake,

in Sec. IV we give a brief overview of the statistical exchange arising in fermionic and bosonic chains. In Sec. V, we describe the propagation dynamics of classical wave packets in these same systems. Finally, conclusions are drawn in Sec. VI.

### II. SINGLE-SITE EXCITATION DYNAMICS

In the present photonic lattice systems the quantum bits correspond to waveguide sites, and the two allowed states for each qubit are “occupied” ( $|1\rangle$ ) or “unoccupied” ( $|0\rangle$ ) depending on whether a photon is “present” or “absent” at such a waveguide site. For instance, a spin chain containing  $N$  elements in the state  $|\xi\rangle = |\downarrow_1 \downarrow_2 \cdots \uparrow_n \cdots \downarrow_N\rangle$ , in which the spin at the  $n$ th site has been flipped from its ground state  $|0_n\rangle = |\downarrow_n\rangle$  to the state  $|1_n\rangle = |\uparrow_n\rangle$ , is represented by the photon-encoded state  $|\xi\rangle = |0_1 0_2 \cdots 1_n \cdots 0_N\rangle$  where a single photon is present at the  $n$ th site of a photonic lattice having  $N$  waveguide elements; see Figs. 1(a) and 1(b). As a result, the physical process of quantum-state transfer in waveguide lattices can be understood as a dynamical translation of any localized single-photon wave function from the input port to another wave function at the output port. In other words, in such a photonic lattice, any initial one-site excitation state is expected to be transferred from qubit  $n$  to qubit  $N - n + 1$ , as illustrated in Fig. 1(b).

In order to achieve perfect transfer of photon-encoded quantum states, an array of evanescently coupled waveguides is used having a parabolic law distribution for the coupling coefficients between nearest-neighbor elements [5]. To do so, we first establish a one-to-one correspondence between the interchannel coupling coefficients of the waveguide lattice and the matrix elements of the quantum-mechanical angular momentum operator  $J_x$ :

$$(J_x)_{m,n} = \frac{1}{2} [\sqrt{(j-m)(j+m+1)}\delta_{n,m+1} + \sqrt{(j+m)(j-m+1)}\delta_{n,m-1}]. \quad (1)$$

Thus, the coupling matrix must be tridiagonal with elements  $(J_x)_{m,n} \neq 0$  if  $|m-n| \leq 1$ , and  $(J_x)_{m,n} = 0$  otherwise. The dimension of the  $J_x$  matrix is  $N = 2j + 1$ , and the indices  $m, n$  range from  $-j$  to  $j$  in unit steps, and  $j$  is a positive integer or half integer [15]. In order to map the matrix elements of the  $J_x$  operator over the coupling coefficients of the proposed photonic lattice, we define the function  $f(n) = \frac{1}{2}\sqrt{(N-n)n}$

\*Corresponding author: aleija@creol.ucf.edu

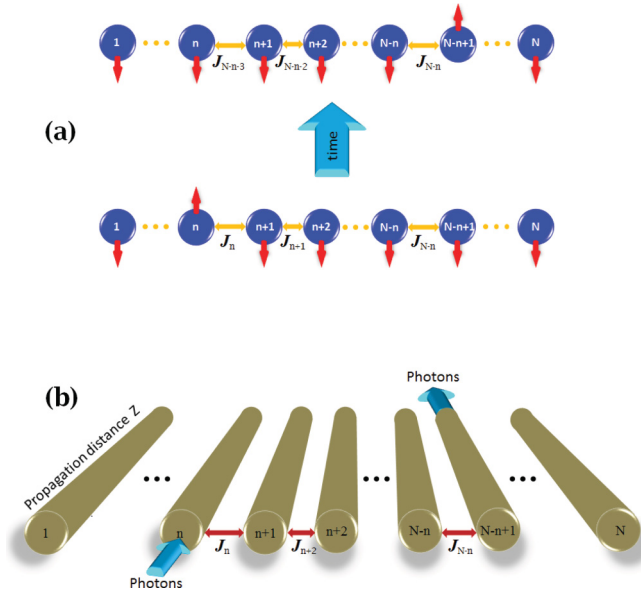


FIG. 1. (Color online) (a) Schematic of a spin chain containing  $N$  spin  $1/2$  particles with hopping rate  $J_n$  between nearest neighbors. The  $n$ th particle has been flipped from its ground state  $|\downarrow_n\rangle$  to the state  $|\uparrow_n\rangle$ . (b) In the optical domain this spin system can be represented by photons being launched into the first waveguide element of an array of  $N$  optical waveguides with evanescent nearest-neighbor coupling  $J_n$ .

for the coupling strength between the waveguide element  $n$  and  $(n + 1)$ . Starting from these assumptions one can obtain a set of Heisenberg equations governing the evolution of the single-photon creation operators,

$$i \frac{da_1^\dagger}{dZ} = F(1)a_2^\dagger, \quad (2a)$$

$$i \frac{da_n^\dagger}{dZ} = f(n)a_{n+1}^\dagger + f(n-1)a_{n-1}^\dagger, \quad (2b)$$

$$i \frac{da_N^\dagger}{dZ} = f(N-1)a_{N-1}^\dagger. \quad (2c)$$

Equations (2a) and (2c) describe the quantum dynamics at the boundary waveguides ( $n = 1, N$ ), while Eq. (2b) stands for any other intermediate site. To obtain the solution of these equations we first explore the corresponding eigenvalue problem,  $J_x u^{(m)} = \beta_m u^{(m)}$ , which can be cast as a difference equation:

$$\sqrt{(N-n+1)(n-1)}u_{n-1}^{(m)} + \sqrt{(N-n)n}u_{n+1}^{(m)} = 2\beta_m u_n^{(m)}, \quad (3)$$

where  $\beta_m$  is the  $m$ th propagation eigenvalue of the waveguides, and the boundary condition to satisfy is  $u_0^{(m)} = u_{N+1}^{(m)} = 0$ . A direct calculation reveals that Eq. (3) allows the lattice eigenvectors  $|u^{(m)}\rangle$  whose  $n$ th component is given by

$$u_n^{(m)} = 2^{-\frac{1}{2}(N+1)+n} \sqrt{\frac{(n-1)!(N-n)!}{(m-1)!(N-m)!}} P_{n-1}^{(m-n, N-m-n+1)}(0), \quad (4)$$

while the eigenvalues  $\beta_m$ , as expected from quantum theory, are equidistant integers or half integers in the interval

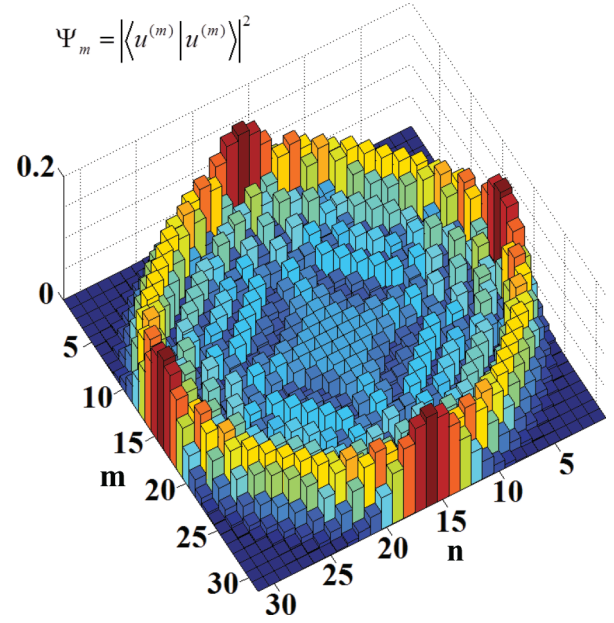


FIG. 2. (Color online) Analytical eigenvector density  $\Psi_m = |\langle u^{(m)} | u^{(m)} \rangle|^2$ . Label  $m$  represents the eigenvector number and  $n$  the corresponding components. Note that unlike standard angular momentum notation we have displaced the origin of  $m, n$  from  $-j$  to  $1$ .

$-(N-1)/2 \leq \beta_m \leq (N-1)/2$  depending on whether  $N$  is odd or even. In Eq. (4),  $P_{n-1}^{(m-n, N+1-m-n)}(0)$  represents the Jacobi polynomials of order  $(n-1)$ , evaluated at the origin and in this case  $n \in [1, N]$ . A useful representation of the entire eigenvector basis is provided by a density plot of the matrix  $\Psi_m = |\langle u^{(m)} | u^{(m)} \rangle|^2$ , shown in Fig. 2 for a lattice of 31 waveguides. Note that this matrix is symmetric across the diagonal. Using the eigenvectors given in Eq. (4) and the corresponding eigenvalues, one can readily obtain the probability amplitudes over the entire lattice at any distance  $Z$ , i.e.,

$$|\psi(Z)\rangle = \sum_{r=1}^N C_r |u^{(r)}\rangle \exp(i\lambda_r Z), \quad (5)$$

where  $C_r = \langle u^{(r)} | \psi(0) \rangle$ . By using Eq. (5), one can show that the input-output states are related through the evolution matrix as follows:

$$a_p^\dagger(0) = \sum_{n=1}^N T_{p,n}^*(Z) a_n^\dagger(Z), \quad (6)$$

where  $T_{p,n}^*(Z)$  denotes the Hermitian conjugate of the  $(p, n)$  matrix element within the unitary transformation,

$$T_{p,q}(Z) = \sum_{r=1}^N u_q^{(r)} u_p^{(r)} \exp(i\lambda_r Z). \quad (7)$$

Note that the transfer matrix given by Eq. (7) can also be obtained by evaluating the exponential of the coupling matrix,  $T_{p,q}(Z) = [\exp(iJ_x Z)]_{p,q}$ , which in quantum mechanics represents a rotation operator about the  $x$  axis [15]. Using this quantum rotation picture, or directly from Eq. (7), one can readily foresee the ‘‘arrival site’’ for single photons

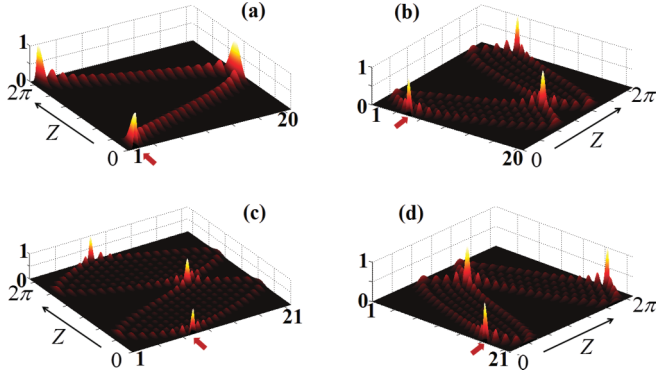


FIG. 3. (Color online) Probability evolution when light is launched into the (a) first, (b) second, (c) eighth, and (d) 17th waveguide. In both lattices the intensity revival distance is at  $z = 2\pi$ .

propagating through these multiport photonic systems. More specifically, using the photon density (photon counting) it is easily found that the probability of detecting a photon at waveguide  $p$ , when launched at  $q$ , is given by  $P_{p,q}(Z) = \langle a_p^\dagger a_p \rangle = |T_{p,q}(Z)|^2$ . Since at distances  $Z = 2\pi S$  ( $S$  being an integer) the matrix elements reduce to  $T_{p,q} = (-1)^S \delta_{pq}$  (for  $N$  even) and to  $T_{p,q} = \delta_{pq}$  (for  $N$  odd), it implies that *collapses* and *revivals* of probability will periodically occur irrespectively of dimensionality  $N$  or of the excitation site. Figure 3 depicts this process for  $J_x$  waveguide arrays with odd and even  $N$ , respectively. These side views clearly indicate that when  $Z = K\pi$  ( $K$  being an *odd* integer), a mirror inversion of the initial quantum probability will occur with respect to the central waveguide. Hence, at these particular distances  $Z = K\pi$  ( $K = \text{odd}$ ), perfect transfer of quantum states is effectively realized.

From Eq. (7) one can also analytically show that for eigenvalues being half integers ( $N = \text{even}$ ), any initial state will exhibit perfect revivals at distances that are multiples of  $4\pi$  ( $Z = 4\pi$ ), whereas for integer eigenvalues ( $N = \text{odd}$ ), revivals occur at multiples of  $Z = 2\pi$ . This is easily understood since at  $Z = 2\pi$  the rotation operator  $T_{p,q}(Z = 2\pi) = [\exp(i2\pi J_x)]_{p,q} = \pm \delta_{p,q}$ , i.e., it is diagonal with elements  $+1$  or  $-1$  depending on whether the corresponding eigenvalues are integers or half integers, respectively. Even more interesting is the fact that perfect revivals, or perfect transfer, of single-photon entangled states are possible in this type of system. To elucidate this, consider for instance the evolution of a multipartite  $W$  state, where a single photon is coherently “shared” among the  $N$  optical modes contained in a  $J_x$  photonic array:

$$|W_N(0)\rangle = \frac{1}{\sqrt{N}}(|10\dots 0\rangle + |01\dots 0\rangle + \dots + |00\dots 1\rangle). \quad (8)$$

Accordingly, the state will evolve to the superposition

$$|\psi(Z)\rangle = \frac{1}{\sqrt{N}}(T_{1,1}|10\dots 0\rangle + \dots + T_{1,N}|00\dots 1\rangle) + \frac{1}{\sqrt{N}}(T_{2,1}|10\dots 0\rangle + \dots + T_{2,N}|00\dots 1\rangle)$$

$$+ \dots + \frac{1}{\sqrt{N}}(T_{N,1}|10\dots 0\rangle + \dots + T_{N,N}|00\dots 1\rangle). \quad (9)$$

Therefore, since  $T_{p,q}(Z = 2\pi) = \pm \delta_{p,q}$  it is obvious that this superposition of states will “collapse” back to the initial multipartite  $W$  state at distances  $Z = n2\pi$  ( $n$  being an integer),

$$|\psi(Z = n2\pi)\rangle = \pm \frac{1}{\sqrt{N}}(|10\dots 0\rangle + |10\dots 0\rangle + \dots + |10\dots 0\rangle), \quad (10)$$

apart from an overall phase. All these arguments along with numerical simulations clearly elucidate the potential and capability of these optical arrangements to effectively achieve a perfect transfer of any arbitrary single-photon quantum state.

Another significant aspect concerning separable single-photon states is the fact that at a distance  $Z = \pi/2$  the probabilities described by the rotation operator,  $|\exp(iJ_x\pi/2)|^2$ , are identical to the matrix density of modes  $\Psi_m = |\langle u^{(m)} | u^{(m)} \rangle|^2$ . In other words, if a single photon is launched into a  $J_x$  photonic lattice at waveguide  $q$ , after propagating a distance  $Z = \pi/2$ , it will be found at site  $p$  with a probability  $|T_{p,q}(\pi/2)|^2 = |u_p^{(q)}|^2$ , where  $u_p^{(q)}$  is an eigenvector of the  $J_x$  matrix given in Eq. (4). As a consequence, the vector components of the evolution operator,  $\exp(iJ_x\pi/2)$ , are orthonormal [16].

### III. PERFECT TRANSFER OF SPATIALLY EXTENDED PATH-ENTANGLED STATES

In what follows we explore the possibility of transferring spatially extended high-entangled photon states via  $J_x$  photonic lattices. To do so, we assume two different configurations for the input states, that is, photon pairs correlated and anticorrelated in their position,

$$|\psi_C\rangle = \frac{1}{\sqrt{2N}}[(a_1^\dagger)^2 + (a_2^\dagger)^2 + \dots + (a_N^\dagger)^2]|0\rangle, \quad (11)$$

$$|\psi_A\rangle = \sqrt{\frac{2}{N}}[a_1^\dagger a_N^\dagger + a_2^\dagger a_{N-1}^\dagger + \dots + a_{\frac{N}{2}}^\dagger a_{\frac{N}{2}+1}^\dagger]|0\rangle.$$

Conceptually, photon pairs with correlated positions, denoted by  $|\psi_C\rangle$ , correspond to the situation where both photons are simultaneously coupled into any waveguide within the entire array with an equal probability. The physical realization of such a state can be achieved by placing the  $J_x$  array immediately after a type I collinear degenerate narrow-band spontaneous parametric down-conversion (SPDC) thin-crystal source [17]. On the other hand, the anticorrelated entangled state corresponds to the case where the photon pair is symmetrically coupled to waveguides on opposite sides of the array. The quantum dynamics of such states is analyzed by monitoring the evolution of the coincidence rate (correlation maps) at the output  $\Gamma_{m,n} = \langle \psi_{A,C} | a_m^\dagger a_n^\dagger a_n a_m | \psi_{A,C} \rangle$ , which gives the probability of finding one photon at waveguide  $m$  and its twin at site  $n$  [9,18]. For the particular examples considered here, the correlation map corresponding to the correlated input state  $|\psi_C\rangle$  is given by  $\Gamma_{m,n} = |\sum_{k=1}^N T_{m,k} T_{n,k}|^2$ , whereas for the anticorrelated one,  $|\psi_A\rangle$ , it becomes  $\Gamma_{m,n} = |\sum_{k=0}^{N-1} T_{m,1+k} T_{n,N-k}|^2$  [19]. In order to examine these effects

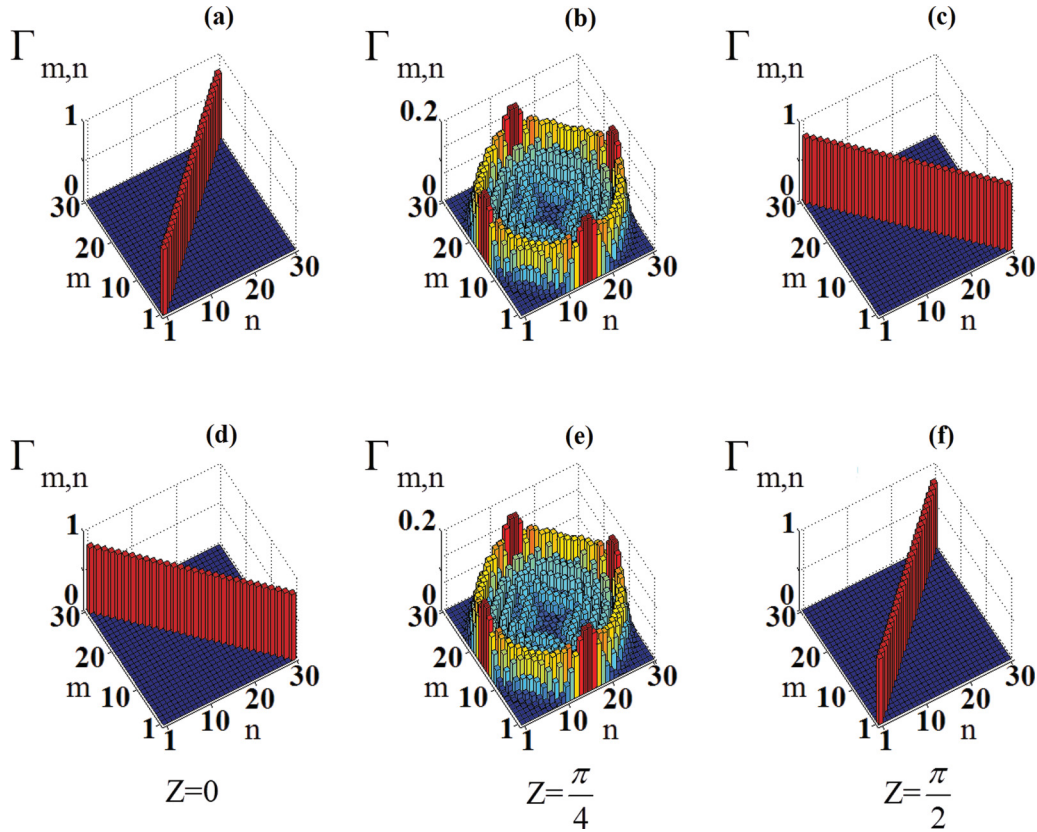


FIG. 4. (Color online) (a)–(c) Upper row shows the calculated quantum correlation maps when the correlated input state  $|\psi_C\rangle$  is coupled into a  $J_x$  photonic lattice. (d)–(f) Similarly, bottom row depicts the correlation evolution for the anticorrelated input state  $|\psi_A\rangle$ .

we assume a  $J_x$  array of  $N = 30$  waveguide elements, which implies half-integer eigenvalues. Thus, exact revivals for any input states are expected to occur at  $Z = 4\pi$ . When the input state is initially correlated, the probability map gradually spreads and eventually becomes circularlike at exactly  $Z = \pi/4$ ; see Fig. 4(b). This circle of probability exhibits four peaks or maxima over the “cardinal points” of the correlation matrix. As a result, both photons will separate and one of them can be found propagating around the boundary sites, whereas its twin could be detected at the center of the lattice. Evidently, in regions between the “cardinal points” both regimes, bunching and antibunching, coexist with an equal probability and the photons can be found either together around the boundaries or separate on opposite sides of the lattice. This region where the probability matrix acquires this peculiar circular shape can be considered as the turning points for the path-entangled states under consideration. Notably, the correlation matrix at a distance  $Z = \pi/4$  is identical to the matrix density of modes given by  $\Psi_m = |\langle u^{(m)} | u^{(m)} \rangle|^2$ , or equivalently to the probability matrix,  $|\exp(iZJ_x)|^2$ , evaluated at  $Z = \pi/2$  which is valid for separable, nonentangled, single-photon states. In the present case, however, we are dealing with entangled two-photon states and therefore such a behavior is exhibited at half the distance, that is, at  $Z = \pi/4$  [20]. Subsequently, after propagating a distance  $Z = \pi/2$  the photons evolve into a perfect anticorrelated state, implying that the two photons

are traveling in opposite directions but symmetrically with respect to the center of the lattice; see Fig. 4(c). This behavior is a direct outcome of the destructive quantum interference between indistinguishable states. In essence, this phenomenon can be thought of as an inverse version of the Hong-Ou-Mandel effect, where two single photons launched into different ports of a 50:50 beam splitter tend to bunch together at the output ports, thus “excluding” by quantum interference the indistinguishable  $|1\rangle|1\rangle$  states [21]. Interestingly, right after a distance  $Z = \pi/2$ , the correlation matrix evolves back to the correlated states  $|\psi_C\rangle$  in a fully reversible way. In other words, the photon correlations form a circle of probability at  $Z = 3\pi/4$ , and the state becomes correlated at  $Z = \pi$ . This effect is obvious since at  $Z = \pi$  the matrix elements  $T_{p,q}$  vanish except for the ones over the diagonal ( $T_{1,N} = T_{2,N-1} = \dots = T_{N,1} = -i$ ) signifying that photon pairs coupled into waveguides located over one side of the lattice will symmetrically emerge from the waveguides on the opposite side, and vice versa.

This picture is, in a way, altered when the initial biphoton state is anticorrelated,  $|\psi_A\rangle$ . Under such circumstances, the correlation matrix again leads to a circle of probability at distances  $Z = \pi/4$  and  $Z = 3\pi/4$  [see Fig. 4(e)], somehow matching the behavior exhibited in the previous case at these same distances. Midway however, the scenario differs and the state becomes fully correlated; see Fig. 4(f). At this point, this implies that both photons will be found traveling together at

the same waveguide site within the array with equal probability as a  $|\psi_C\rangle$  state. As before, at  $Z = \pi$ , a perfect transfer of the initial entangled state is expected to occur.

#### IV. QUANTUM EXCHANGE STATISTICS

In the present work, the photonic lattice has been excited with bosonic particles, whereas in actual spin chains such excitations are fermionic in nature. A fundamental difference between bosons and fermions is the exchange statistics which dictate the corresponding dynamical behavior of the system. In this respect, it is important to compare and analyze the arrival statistics of multiple excitations propagating through fermionic and bosonic systems. To do so, we examine the correlation matrix  $\Gamma_{m,n} = \langle a_m^\dagger a_n^\dagger a_n a_m \rangle$  which measures the probability for a pair of excitations ‘‘arriving’’ at sites  $m$  and  $n$ . In particular we consider the arrival statistics when both arrangements are initialized in the state  $|\psi_{\text{in}}\rangle = a_1^\dagger a_N^\dagger |0\rangle$ , i.e., sites 1 and  $N$  are simultaneously excited. In this case, the probability amplitudes at waveguide  $n$  are given by the matrix elements,

$$\begin{aligned} T_{n,1}(Z) &= \binom{N-1}{n-1}^{1/2} \cos^{N-n} \left( \frac{Z}{2} \right) \sin^{n-1} \left( \frac{Z}{2} \right) (-i)^{n-1} \\ T_{n,N}(Z) &= \binom{N-1}{n-1}^{1/2} \cos^{n-1} \left( \frac{Z}{2} \right) \sin^{N-n} \left( \frac{Z}{2} \right) (-i)^{N-n}. \end{aligned} \quad (12)$$

From these expressions, one can see that the average excitation number at site  $n$ ,  $P_n = \langle a_n^\dagger a_n \rangle = |T_{n,1}|^2 + |T_{n,N}|^2$ , predicts that both particles, either bosons or fermions, are probabilistically expected to collide at  $Z = \pi/2$ , and two-excitation interference occurs. In order to analyze such an interference effect, we compute the correlation matrix  $\Gamma_{m,n} = \langle a_m^\dagger a_n^\dagger a_n a_m \rangle$  at this particular distance,  $Z = \pi/2$ . In the case of a photonic system, the state evolves such that at  $Z = \pi/2$ , the probability of finding excitations at sites  $m$  and  $n$  is given by

$$\Gamma_{m,n} = \begin{cases} 0 & n - m : \text{odd} \\ \frac{1}{2^{2N-4}} \binom{N-1}{m-1} \binom{N-1}{n-1} & n - m : \text{even} \end{cases}. \quad (13)$$

This expression indicates that at the collision distance the correlation vanishes at sites where the difference  $(n - m)$  is an odd number. On the other hand, for a spin-chain, the statistical exchange differs in the sense that now the correlation vanishes at sites where the difference  $(n - m)$  is an even number.

$$\Gamma_{m,n} = \begin{cases} \frac{1}{2^{2N-4}} \binom{N-1}{m-1} \binom{N-1}{n-1} & n - m : \text{odd} \\ 0 & n - m : \text{even} \end{cases}. \quad (14)$$

These effects are illustrated in Fig. 5(a) (bosonic probability) and Figs. 5(b) and 5(c)—correlations for bosons and fermions, respectively. As clearly visible in Fig. 5(b), photons can only be registered in output configurations where the difference of their positions  $n - m$  is even, whereas fermionic excitations can only be registered in output configurations where the difference of their positions is odd.

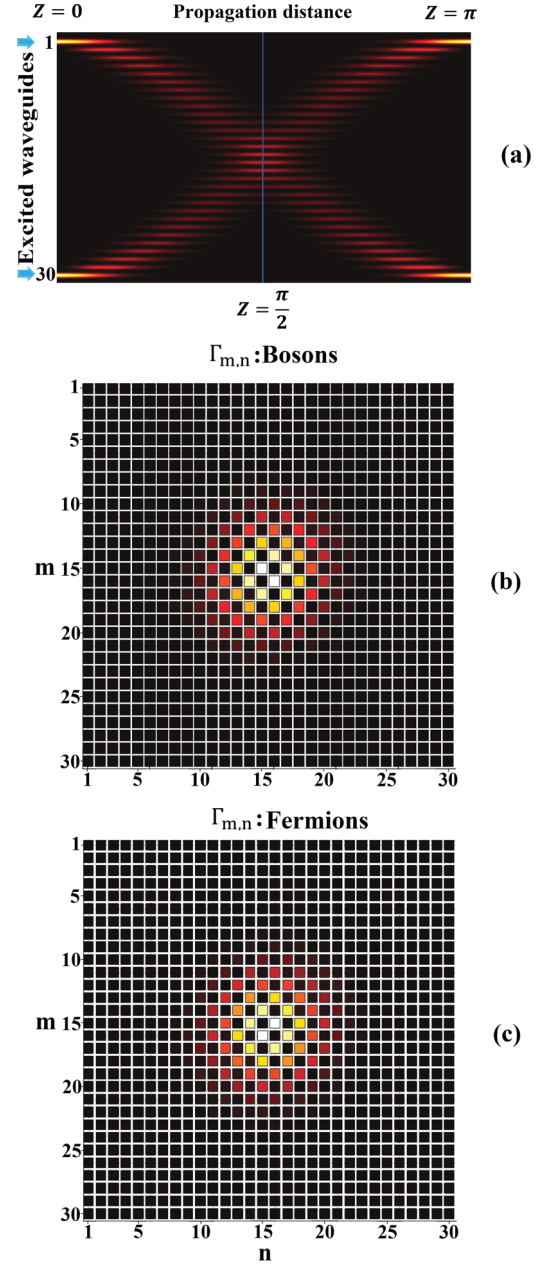


FIG. 5. (Color online) (a) Theoretical average particle number at waveguide  $m$ ,  $\langle n_m(Z) \rangle$ , of two single photons simultaneously launched into the first and last waveguides. The blue line indicates the distance  $Z = \pi/2$ , where the correlation matrix is obtained. (b), (c) Calculated correlation map  $\Gamma_{m,n}$ : As the particles approach the ‘‘collision region’’ ( $Z = \pi/2$ ), the coincidence rate vanishes for the particular combinations  $(n - m) = \text{odd}$ , whereas for fermions it vanishes when  $(n - m) = \text{even}$ .

#### V. CLASSICAL DYNAMICS

In this section we present the propagation dynamics of classical light in the so-called  $J_x$  photonic lattices. It is shown that light traversing such photonic configurations can display interesting features such as Talbot-like revivals and discrete focusing. Before starting it is important to note that if classical light is injected into photonic lattices, as opposed

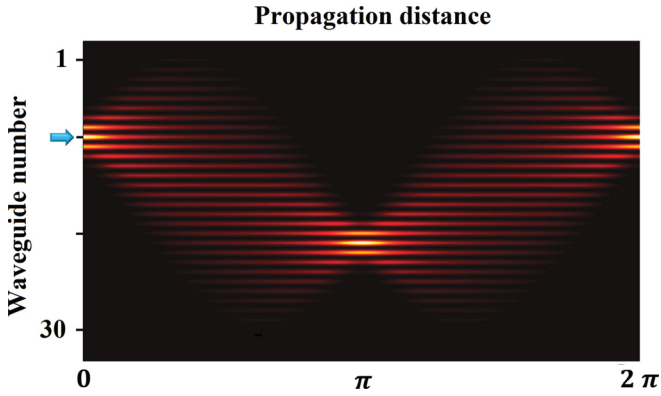


FIG. 6. (Color online) Wave packet dynamics: evolution of a discrete Gaussian beam in a  $J_x$  waveguide array. The blue arrow indicates the waveguide where the wave packet is initially centered.

to single photons, the intensity patterns will be identical to the probability distributions exhibited by single photons [18,22]. Hence, the evolution equations governing classical light propagation in these systems are given by

$$i \frac{dE_1}{dZ} = -f(1)E_2, \quad (15a)$$

$$i \frac{dE_n}{dZ} = -f(n)E_{n+1} - f(n-1)E_{n-1}, \quad (15b)$$

$$i \frac{dE_N}{dZ} = -f(N-1)E_{N-1}, \quad (15c)$$

where again  $f(n) = \frac{1}{2}\sqrt{(N-n)n}$  [23]. Given that the interaction matrix in this case is identical to the coupling matrix in the Heisenberg equations (2) (apart from a negative sign), the eigensolutions and eigenvalues remain the same as in the previous case, as given by Eq. (4). As previously indicated and illustrated in the first part of this work, the impulse response of this type of lattice exhibits Talbot-like revivals. In fact, since any initial condition can be described via a superposition of single-channel excitations, such revivals can occur for any input field. For instance, if we inject a Gaussian wave packet, centered around site  $n$ , it will first spread among the guides and eventually will expand within the array at  $Z = \pi/2$ ; see Fig. 6. Subsequently at  $Z = \pi$ , the wave packet contracts and returns to its initial form but now with its center shifted at site  $N - n$ . In other words, at this particular distance a mirror inversion of the input field is produced. After passing this middle cycle point, light again spreads out and perfect revivals are observed at  $Z = 2\pi$ . These periodicities are, of course, the outcome of coherent interference. On the other hand, when equal-amplitude light is coupled into several waveguides it will give rise to a richer dynamics, which in principle can be exploited in order to combine most of the incident power in a single output channel. Unlike some other proposed techniques to realize discrete focusing of light, the present approach is achieved without any phase modulation of the input field; see, for instance, Refs. [24,25]. To exemplify the focusing process in Fig. 7 we present theoretical results concerning propagation arising from a gradual filling of the input channels of a  $J_x$

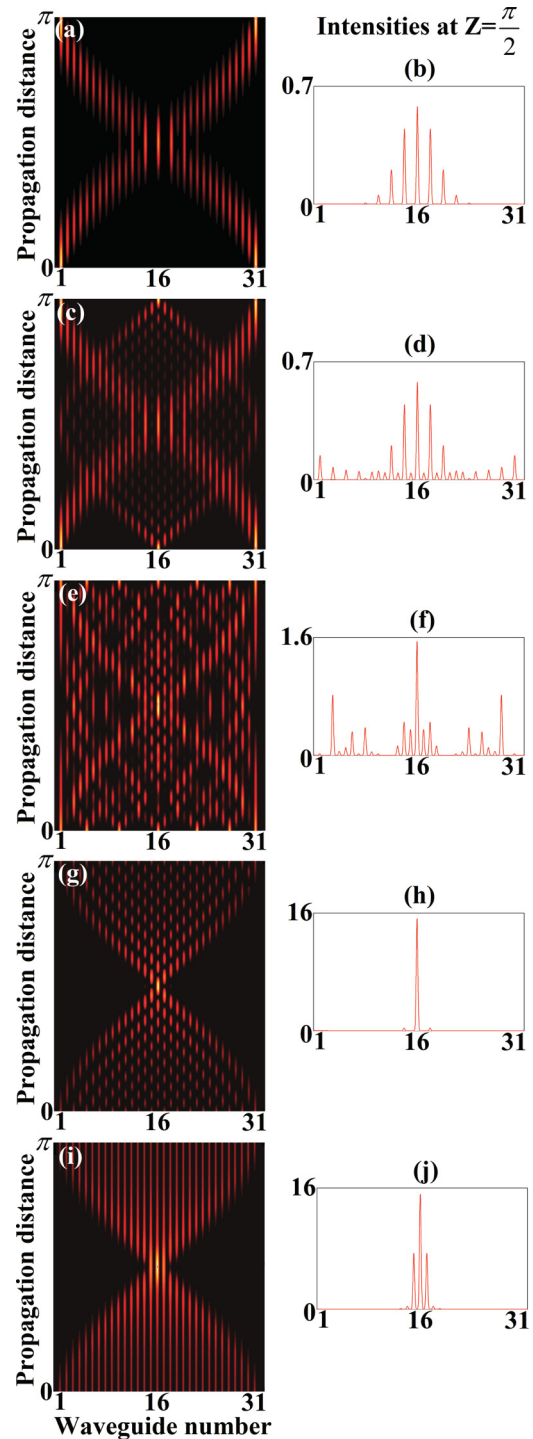


FIG. 7. (Color online) Left column depicts the calculated intensity propagation when light is launched into (a) the first and 31st sites, (c) the first, 16th, and 31st sites, (e) the first, fifth, tenth, 16th, 22nd, 27th, and 31st sites, (g) every other site ( $n = \text{odd}$ ), and (i) every site. In all the cases we have considered unitary input intensities at every excited waveguide. Right column shows the intensity distributions at  $Z = \frac{\pi}{2}$  for each case.

array containing 31 waveguides. For the case where only the first and last waveguide channels are excited, the superposition of the propagating fields at  $Z = \pi/2$  is analytically

described by

$$E_n \left( Z = \frac{\pi}{2} \right) = \begin{cases} -i2 \left( \frac{1}{\sqrt{2}} \right)^{N-1} \sqrt{\frac{(N-1)!}{(n-1)!(N-n)!}} \cos \left( \frac{n\pi}{2} \right), \Leftrightarrow (-i)^N = i \\ i2 \left( \frac{1}{\sqrt{2}} \right)^{N-1} \sqrt{\frac{(N-1)!}{(n-1)!(N-n)!}} \sin \left( \frac{n\pi}{2} \right), \Leftrightarrow (-i)^N = -i \end{cases} \quad (16)$$

Note that the upper row stands for the particular case illustrated here,  $N = 31$ . From expressions (16) one can readily infer that the field will vanish, because of interference, in  $(N + 1)/2$  sites when  $(-i)^N = i$  and in  $(N - 1)/2$  when  $(-i)^N = -i$ . This indicates that light traveling from opposite sides of the  $J_x$  array will acquire site-dependent phases which leads to destructive interference at some lattice sites and constructive in other positions. In Fig. 7(a) the intensity evolution is shown for this particular case, whereas Fig. 7(b) depicts the corresponding intensity at distance  $Z = \pi/2$ . In similar fashion one can show that by increasing the number of excitation channels, most of the incoming light can be directed towards the central waveguide as shown in Figs. 7(c), 7(e), 7(g), and 7(i). For the special case of light coupled into the entire array, energy symmetrically concentrates into seven lattice sites at the center of the array collecting just 50% of the total power at the

central guide; see Figs. 7(i) and 7(j). On the other hand, if light is injected into alternated sites, the focusing scheme becomes more efficient delivering 95% of the power at the central waveguide, and just 2.5% to its adjacent neighbors. Figures 7(g) and 7(h) illustrate this process.

## VI. CONCLUSION

In conclusion, we have shown that a certain class of waveguide arrays—the so-called  $J_x$  photonic lattices—can be used as a method for perfect transfer of separable and entangled quantum states. In these systems, revivals of quantum probability as well as classical intensity are possible—each could lead to interesting applications. In essence, we have exploited the formal analogy between optical waveguide arrays and Heisenberg spin chains to bring the idea of perfect state transfer into the quantum optical realm. Using the well-known theory of quantum angular momentum and rotation operators, we have demonstrated perfect revivals, both quantum and classical, which can be analytically described in one-dimensional photonic lattices composed of evanescently coupled waveguides. Our results may be of importance in extending the physics of spin chains to the classical and quantum optical domain, leading to interesting new photonic applications.

- 
- [1] S. Bose, *Phys. Rev. Lett.* **91**, 207901 (2003).
- [2] E. Pazy, E. Biolatti, T. Calarco, I. D’Amico, P. Zanardi, F. Rossi, and P. Zoller, *Europhys. Lett.* **62**, 175 (2003).
- [3] J. I. Cirac, P. Zoller, H. J. Kimble, and H. Mabuchi, *Phys. Rev. Lett.* **78**, 3221 (1997).
- [4] S. Ritter, C. Nölleke, C. Hahn, A. Reiserer, A. Neuzner, M. Uphoff, M. Mücke, E. Figueroa, J. Bochmann, and G. Rempe, *Nature* **484**, 195 (2012).
- [5] M. Christandl, N. Datta, A. Ekert, and A. J. Landahl, *Phys. Rev. Lett.* **92**, 187902 (2004).
- [6] C. Albanese, M. Christandl, N. Datta, and A. Ekert, *Phys. Rev. Lett.* **93**, 230502 (2004).
- [7] D. P. DiVincenzo, D. Bacon, J. Kempe, G. Burkard, and K. B. Whaley, *Nature (London)* **408**, 339 (2000).
- [8] G. Benenti, G. Casati, and G. Strini, *Principles of Quantum Computation and Information* (Scientific World, Singapore, 2007).
- [9] J. O. Owens, M. A. Broome, D. N. Biggerstaff, M. E. Goggin, A. Fedrizzi, T. Linjordet, M. Ams, G. D. Marshall, J. Twamley, M. J. Withford, and A. G. White, *New J. Phys.* **13**, 075003 (2011).
- [10] I. L. Garanovich, S. Longhi, A. A. Sukhorukova, and Y. S. Kivshar, *Phys. Rep.* **518**, 1 (2012).
- [11] R. Keil, A. Perez-Leija, F. Dreisow, M. Heinrich, H. Moya-Cessa, S. Nolte, D. N. Christodoulides, and A. Szameit, *Phys. Rev. Lett.* **107**, 103601 (2011).
- [12] R. Keil, A. Perez-Leija, P. Aleahmad, H. Moya-Cessa, S. Nolte, D. N. Christodoulides, and A. Szameit, *Opt. Lett.* **37**, 3801 (2012).
- [13] D. N. Christodoulides, F. Lederer, and Y. Silberberg, *Nature* **424**, 817 (2003).
- [14] A. Crespi, S. Longhi, and R. Osellame, *Phys. Rev. Lett.* **108**, 163601 (2012).
- [15] A. Messiah, *Quantum Mechanics* (Dover Publications, New York, 1999).
- [16] J. D. Jackson, *Mathematics for Quantum Mechanics* (Dover Publications, New York, 1990).
- [17] Y. H. Shih and C. O. Alley, *Phys. Rev. Lett.* **61**, 2921 (1988).
- [18] Y. Bromberg, Y. Lahini, R. Morandotti, and Y. Silberberg, *Phys. Rev. Lett.* **102**, 253904 (2009).
- [19] A. Perez-Leija, R. Keil, A. Szameit, A. F. Abouraddy, H. Moya-Cessa, and D. N. Christodoulides, *Phys. Rev. A* **85**, 013848 (2012).
- [20] Y. Bromberg, Y. Lahini, and Y. Silberberg, *Phys. Rev. Lett.* **105**, 263604 (2010).
- [21] C. K. Hong, Z. Y. Ou, and L. Mandel, *Phys. Rev. Lett.* **59**, 2044 (1987).
- [22] W. K. Lai, V. Buek, and P. L. Knight, *Phys. Rev. A* **43**, 6323 (1991).
- [23] R. Gordon, *Opt. Lett.* **29**, 2752 (2004).
- [24] I. D. Chremmos and N. K. Efremidis, *Phys. Rev. A* **85**, 063830 (2012).
- [25] E. Suran, F. Louradour, A. Barthelemy, A. Kudlinski, G. Martinelli, Y. Quiquempois, and M. Douay, *Opt. Lett.* **34**, 2536 (2009).